

# Pinch Points and Kasteleyn Transitions: How Spin Ice Changes its Entropy

T. Fennell<sup>1,2</sup>, S. T. Bramwell<sup>1,3</sup>, D. F. McMorrow<sup>1,2,4</sup> P. Manuel<sup>4</sup>

<sup>1</sup>London Centre for Nanotechnology, 2-16 Torrington Place, London WC1E 7HN, UK; <sup>2</sup>Department of Physics, University College London, Gower Street, London, WC1E 6BT, UK; <sup>3</sup>Department of Chemistry, University College London, 20 Gordon Street, London WC1H 0AJ, UK; <sup>4</sup>ISIS Facility, Rutherford Appleton Laboratory, Chilton, Didcot, Oxon, OX11 0QX, UK

Complex disordered states - from liquids and glasses to exotic quantum matter - are ubiquitous in nature. Their key properties include finite entropy, power-law correlations and emergent organising principles. In spin ice, spin correlations are determined by an ice rules organising principle that stabilises a magnetic state with the same zero point entropy as water ice. The entropy can be manipulated with great precision by a magnetic field: with field parallel to the trigonal axis one obtains quasi two dimensional kagome ice which can be mapped onto a dimer model. Here we use a field tilted slightly away from the trigonal axis to control the dimer statistical weights and realise the unusual critical behaviour predicted by Kasteleyn. Neutron scattering on  $\text{Ho}_2\text{Ti}_2\text{O}_7$  reveals pinch point scattering that characterises the emergent gauge structure of kagome ice; diffuse peaks that shift with field, signaling the Kasteleyn physics; and an unusual critical point.

In spin ice materials such as  $\text{Ho}_2\text{Ti}_2\text{O}_7$  and  $\text{Dy}_2\text{Ti}_2\text{O}_7$  [1-6], the Ising-like rare earth spins are analogous to hydrogen displacement vectors in water ice, so the statistical mechanics of these materials may be mapped directly onto Pauling’s model of hydrogen disorder in water ice. The ground state organising principle, or “ice rule” is that two spins should point into and two out of each elementary tetrahedron of the lattice occupied by Ho or Dy (Fig. 1a and b). This rule does not enforce long-range spin order and spin ice shares with water ice the Pauling zero point entropy [2,7]. A magnetic field directed along the trigonal axis (Fig. 1b) “pins” one spin per tetrahedron along the field direction, but, provided that it is not too strong, allows the ice rules to dictate that the other three spins per tetrahedron must be organised into “two-out-one-in” (for an “up” tetrahedron as pictured). As first observed by Matsuhira et al. [4], this modified ice rule results in a reduced, but still well-defined, zero point entropy. The spins carrying this entropy are arranged in decoupled two-dimensional sheets with kagome geometry, hence the name “kagome ice” [4]. Application of a stronger field breaks the ice rule to enforce an ordered “one-in-three-out” arrangement, giving the magnetization a two plateau form (Fig. 1b and c). This process is accompanied by a giant spike in the residual entropy [8,9]. The entropy spike is due to the crossing of an extensive number of levels which have macroscopic entropies: at the critical field all possible kagome ice states, one-in-three-out states and combinations of the two, have the same energy as the field exactly balances the interactions [7]. This process, predicted by Bonner and Fisher [10], is anticipated to be general for any Ising antiferromagnet but remains largely uninvestigated experimentally.

The properties of the spin ice materials have attracted much theoretical interest. In spin ice the ice rules have been shown to arise as a many body effect of the dipolar interaction between magnetic moments [11-14]. What is remarkable about spin ice is that the ice rules emerge from the dipolar interaction, but in other cases an effective dipolar interaction may emerge from ice rules stabilised

by local interactions as in the case of water ice or the near neighbour antiferromagnet [7,15]. In either situation the key experimental signatures are “pinch point” singularities in the static scattering function  $S(\mathbf{Q})$  [13,16,17]. Because ice rules are a “Gauss’s law” or divergence free local constraint, they can generally stabilise spin patterns that are analogous to magnetic or electric field interactions, which means that longitudinal magnetization fluctuations are completely suppressed: a so-called “emergent gauge structure”. This produces the pinch point scattering, which is singular in one direction and diffuse in all others. Well defined pinch points have previously been observed in ferroelectric systems like KDP [18] where  $S(\mathbf{Q})$  is a measure of the local polarization fluctuations. However, they are less well defined in candidate magnetic systems like  $\text{CsNiCrF}_6$  [19],  $(\text{Y}_{1-x}\text{Sc}_x)\text{Mn}_2$  [20] and spin ice in zero field [21,22]. Our observation of them (described below) may be the first clear example in magnetism.

Moessner and Sondhi showed that the kagome ice phase can be mapped to the dimer model on the hexagonal lattice [23]. Every triangle of the kagome lattice has two spins with positive projection on the field and one opposed to the field. If the kagome lattice is replaced by its hexagonal dual and the bonds centered on a field-opposing spin are coloured, a kagome ice state becomes a disordered dimer state on the hexagonal lattice, as illustrated in Fig. 1a. The dimer model on the hexagonal lattice was originally studied by Kasteleyn [24], who showed that the dimer correlations are critical. Three dimer orientations are available and Kasteleyn found a triangular phase diagram depending on their statistical weights  $Z_1$ ,  $Z_2$  and  $Z_3$  (Fig. 1d). When  $Z_1 > Z_2 = Z_3$  (for example), the first dimer orientation will be selected and there will be a transition to a long range ordered dimer solid. This so-called Kasteleyn transition has many remarkable properties, elucidated by Moessner and Sondhi [23], including an asymmetric first/second order appearance (as yet unobserved in experiment). In kagome ice it is expected that small tilts of the field close to the [111] axis will be equivalent to tuning the statistical weights of the dimer orientations [23].

We performed neutron scattering experiments on holmium titanate,  $\text{Ho}_2\text{Ti}_2\text{O}_7$ . Although detailed bulk measurements of the  $[111]$  field direction have mainly been performed on dysprosium titanate,  $\text{Dy}_2\text{Ti}_2\text{O}_7$ , the holmium material lends itself much better to neutron scattering and it is expected to show qualitatively the same behaviour. In general, the diffuse neutron scattering is a direct measure of  $S(\mathbf{Q})$ , the Fourier transformed spin-spin correlation function: it would show resolution limited Bragg peaks for long range order, broad diffuse peaks for short range order and sharp, but non-resolution limited peaks for critical scattering. Fig. 1c shows the evolution of the  $(0, \bar{2}, 2)$  magnetic Bragg peak intensity of  $\text{Ho}_2\text{Ti}_2\text{O}_7$  as a function of field. This quantity shows a similar two plateau structure to the bulk magnetization [25] with the lower plateau corresponding to the kagome ice phase. Fig. 2a, c and e show the corresponding neutron scattering patterns in the plane of reciprocal space perpendicular to  $[111]$  in zero field, in the kagome ice plateau and at the termination of the plateau respectively. In the kagome ice phase the diffuse scattering compares quite well with a simulation of the near neighbour spin ice model (Fig. 2c), with two broad peaks and a saddle point at to  $(\bar{1}, \bar{1}, 2)$  and striking pinch point singularities at  $(\frac{2}{3}, \frac{2}{3}, \frac{4}{3})$  and  $(\frac{4}{3}, \frac{4}{3}, \frac{8}{3})$ . The position of the pinch points corresponds to the zone centers of a  $\mathbf{Q} = 0$  cell in the kagome plane. Proof that these are indeed pinch points in the manner discussed in Refs. 13, 16, and 17 is given in Fig. 3. Such pinch points are a direct signature of a state governed by ice-rules or an emergent gauge structure. The remarkable feature is the ease with which these pinch points can be detected. They are explicitly expected to appear in the  $S(\mathbf{Q})$  of spin ice [13,14] but have not been observed in experiment [21,22], leading to suggestions that they are hidden by other features or too weak to detect at finite temperature. Here the pinch points are extremely clear, posing the question of how ice rule governed spin correlations are modified on dimensional reduction. Very recently Tabata *et al* [26] have published a neutron scattering study of  $\text{Dy}_2\text{Ti}_2\text{O}_7$  with field parallel to  $[111]$  and apparently zero tilt. Within

the constraint of the strong neutron absorption by Dy they are able to confirm the existence of the kagome ice phase, but their data lacks the resolution to test for pinch point singularities or the other physics revealed in our study of  $\text{Ho}_2\text{Ti}_2\text{O}_7$ .

We next discuss the Kasteleyn physics. In order to observe the Kasteleyn transition as described by Moessner and Sondhi [23], one must tilt the field toward [112]. Considering an “up” tetrahedron, with [111] vertical, this corresponds to increasing the effective field at two sites. The remaining site will preferentially carry the “in” spin or dimer. Tilting the field therefore corresponds to tuning the statistical weights of dimer orientations in Kasteleyn’s model, as described above (i.e.  $Z_1 > Z_2 = Z_3$ ). In this situation it is expected that as a function of tilt, the broad peaks would drift away from their positions toward the  $(0, \bar{2}, 2)$  and  $(\bar{2}, 0, 2)$  positions, reaching the zone centers at the transition. On the Kasteleyn phase diagram (Fig. 1d), tilt toward [112] crosses a phase boundary into a dimer solid phase. The selection of a single dimer orientation simultaneously on every stacked kagome layer must therefore generate long range order, in this case equivalent to the  $Q = 0$  order observed with the field parallel to [001], in which magnetic Bragg scattering is observed only at the zone centers [1,27].

If the tilt is toward [110], dimer weights are still altered. In this case the single spin selected will preferentially maintain a positive projection on the field direction. This is equivalent to excluding dimer occupation from this site, or  $Z_1 < Z_2 = Z_3$ . On the Kasteleyn phase diagram, tilting toward [110] crosses the point at which two dimer solids meet. The dimer phase formed is partially ordered with uncorrelated chains of either of the two possible dimer orientations. In spin language, this corresponds to the  $\mathbf{Q} = X$  partial order previously studied in both  $\text{Ho}_2\text{Ti}_2\text{O}_7$  and  $\text{Dy}_2\text{Ti}_2\text{O}_7$  [27]. The tilted field creates an in-out pair from two spins which form a chain, the ice rules form in-out chains from the remaining spins.

The tuning of dimer weights goes approximately as  $\phi B/T$  ( $\phi$  is the tilt angle) so from a position close to the center of the critical phase, one can move toward the phase boundaries by increasing field or tilt, or lowering temperature. Our study is at fixed tilt of about  $1^\circ$  toward  $[110]$  and we vary the field (which is applied approximately parallel to  $[1.05 \ 1.03 \ 1]$ ). In Fig. 4 we compare the scattering at 0.2, 0.5, 1.0 and 1.6 T and see that the split peaks sharpen and move inward, a clear signature of the Kasteleyn tuning of the critical phase. This is also manifested in the Bragg intensity (Fig. 1c), which decreases slightly across the plateau as a function of  $B$ . This is due to the preferential location of the “in” spin at a particular site. Monte Carlo simulations of the nearest neighbour spin ice model with varying tilt toward  $[110]$ , confirm that the peaks drift inward toward the  $(\bar{1}, \bar{1}, 2)$  when the tilt is in this sense (Fig. 4b). In the nearest neighbour model the chains are not coupled, hence only one dimensional order is achieved a rod of scattering appears, but it is known in the real systems that highly anisotropic partial order appears, with non-resolution limited features appearing at  $\mathbf{Q} = X$  positions such as  $(\bar{1}, \bar{1}, 2)$  [27]. Although we have observed a key signature of Kasteleyn’s predictions, we have not explicitly observed the transition. However, the coincident long range or partial order according to tilt direction, and their manifestation at different wavevectors promises a very clear method by which this can be achieved.

An applied field of 1.6 T corresponds to the transition region between the two magnetization plateaus where the “two-in-two-out” rule is broken and one expects a giant entropy spike [7,8]. In  $\text{Dy}_2\text{Ti}_2\text{O}_7$  [6], though not in the nearest neighbour model, this transition takes the form of a line of first order phase transitions terminating in a critical end point on the field ( $B$ ) versus temperature ( $T$ ) phase diagram (Fig. 1b). The experimental entropy peaks along this line and reaches a maximum at the end point. We find, for  $\text{Ho}_2\text{Ti}_2\text{O}_7$ , an anomalous growth in neutron scattering at the point  $(\bar{1}, \bar{1}, 2)$  that peaks near to the expected first order line where it completely swamps the remnants of the kagome ice

scattering (see Figs. 3 and 5). This scattering is relatively sharp in reciprocal space although never a Bragg peak: it closely resembles critical scattering. It possibly indicates the chain state discussed above, but does not seem to depend on tilt, associating it more probably with the transition to the “one-in-three-out” state that terminates the plateau. Indeed, it behaves much like the expected entropy, having a strong peak at a single  $B, T$  point (Fig. 5). These features strongly suggest a critical point at  $B \approx 1.6$  T,  $T = 0.35$  K,  $\mathbf{Q} = (\bar{1}, \bar{1}, 2)$ . Above  $T_c = 0.35$  K the intensity at  $\bar{1}, \bar{1}, 2$  is continuously growing as the field is scanned across the plateau, but below  $T_c$  the intensity in the plateau is independent of field until close to 1.6 T, when there is a sharp onset of the transition.

This critical point is unusual. At a normal critical point, one would expect critical scattering to precede the development of long range order with a Bragg peak at the same, ordering wavevector. In the expected symmetry sustaining transition, critical scattering near to the  $\mathbf{Q} = 0$  positions should accompany changes in Bragg peak intensity at these positions. However, we see strong critical scattering only at the antiferromagnetic wavevector  $(\bar{1}, \bar{1}, 2)$  and in no part of the  $(B, T)$  phase diagram do we see a Bragg peak develop at this position. Why an antiferromagnetic ordering wavevector should go critical, remains, for the time being, a mystery, but the correlation of the  $(\bar{1}, \bar{1}, 2)$  peak with the expected entropy suggests an association of these two properties. Entropy peaks are a general feature of Ising model systems and result from extra degeneracies that are introduced when the field just balances local interactions [9,8,23]. The extra degeneracy corresponds to extra spin configurations added to the manifold of thermally accessible states: here it appears that these configurations are locally antiferromagnetic.

To summarize our results, we have observed the long sought pinch points, characteristic of an ice rules governed magnet. These lie at the zone centers of a  $Q = 0$  cell in the kagome plane. It is a fascinating challenge for theorists to resolve their apparent absence in three dimensional spin ice, with their pres-

ence in two dimensional kagome ice. We have observed the first experimental signature of Kasteleyn’s tunable dimer critical phase, uncovered a new type of dimer ordering that can be realized by this mechanism, and demonstrated an open route to the realization of the full Kasteleyn transition. Finally we have observed an unusual critical point, at which the critical wavevector does not reflect the developing long range order.

In conclusion, the concept of spin ice is relevant to a wide variety of highly correlated systems, including frustrated magnets [16,28,29,30], disordered magnets [31], anomalous metals [32], nanomagnetic arrays [33] and ice itself (which has been described as a highly correlated proton system) [34]. With a field applied along [111], spin ice exhibits some generic phenomena. For example, first order lines with critical end points play an important role in metal-insulator transitions [35] and ferroelectric response [36], while partially ordered phases on the kagome lattice are also predicted for systems of bosons [37]. Our neutron scattering investigation of holmium titanate’s kagome ice plateau has thus revealed a detailed microscopic picture of the statistical physics of a model system that has broad relevance to many aspects of the physics of complex disorder.

**Methods:** A flux-grown single crystal of  $\text{Ho}_2\text{Ti}_2\text{O}_7$  of dimensions  $3 \times 10 \times 15$  mm was aligned with the [111] axis vertical. In this orientation the scattering plane has threefold symmetry and is spanned by the orthogonal sets of vectors  $(\bar{h}, \bar{h}, 2h)$  and  $(\bar{h}, h, 0)$ . The crystal was mounted on a dilution refrigerator insert in a 7 T vertical field cryomagnet. The PRISMA spectrometer at the ISIS facility was used in diffraction mode to map the scattering plane or to make rocking scans about the high symmetry directions (as in [20]). Optimization of the scattering plane while monitoring the intensity of  $(\bar{2}, \bar{2}, 4)$  and  $(2, \bar{2}, 0)$  shows that these axes are tilted  $2^\circ$  above and  $1^\circ$  below the scattering plane respectively. This corresponds to an applied field approximately parallel to



$[1.05 \ 1.03 \ 1]$ , a small tilt toward the  $[110]$ . The near neighbour spin ice model was simulated using a standard Metropolis algorithm. The system size was  $10 \times 10 \times 10$  pyrochlore unit cells. The system was cooled stepwise to low temperature to ensure equilibration in the spin ice manifold, 40000 Monte Carlo steps per spin were used at each temperature for equilibration, followed by 200000 Monte Carlo steps per spin for accumulating thermodynamic quantities, which were sampled every 10000 steps. A series of five such simulations with different seed configurations were averaged. The tilted fields were introduced as  $\mathbf{B} = B(\cos \phi [111]/\sqrt{3} + \sin \phi [\bar{1}\bar{1}2]/\sqrt{6})$ , either at fixed  $\phi$  throughout, or by stepping  $\phi$  at fixed  $B$ .

**Acknowledgements:** It is a pleasure to acknowledge sample environment team at ISIS (in particular R. Down and J. Keeping) and we would like to thank A.S. Wills and R. Moessner for valuable discussions. We thank the EPSRC (UK) for funding.

## References

- [1] Harris, M. J., Bramwell, S. T., McMorrow, D. F., Zeiske, T., Godfrey, K. W., Geometric Frustration in the Ferromagnetic Pyrochlore  $\text{Ho}_2\text{Ti}_2\text{O}_7$ , *Phys. Rev. Lett.* **79**, 2554 (1997).
- [2] Ramirez, A. P., Hayashi A., Cava, R. J., Siddharthan R. & Shastry, B. S. Zero-point entropy in ‘spin ice’. *Nature* **399**, 333 (1999).
- [3] Snyder, J., Slusky, J. S., Cava, R. J. & Schiffer P. How ‘spin ice’ freezes. *Nature* **413**, 48 (2001).
- [4] Matsuhira, K., Hiroi, Z., Tayama, T., Takagi, S. & Sakakibara, T. A new macroscopically degenerate ground state in the spin ice compound  $\text{Dy}_2\text{Ti}_2\text{O}_7$ . *J. Phys. Condens. Matter* **14**, L559 (2002).
- [5] Sakakibara, T., Tayama, T., Hiroi, Z., Matsuhira, K. & Takagi S., Observation of Liquid-Gas-Type Transition in the Pyrochlore Spin Ice Compound  $\text{Dy}_2\text{Ti}_2\text{O}_7$  in a Magnetic Field. *Phys. Rev. Lett.* **90**, 207205 (2003).
- [6] Higashinaka R. & Maeno, Y. Field-Induced Transition of a Triangular Plane in the Spin-Ice Compound  $\text{Dy}_2\text{Ti}_2\text{O}_7$ . *Phys. Rev. Lett.* **95**, 237208 (2005)
- [7] Pauling, L., The Structure and Entropy of Ice and of Other Crystals with Some Randomness of Atomic Arrangement. *J. Am. Chem. Soc.* **57**, 2680 (1935).
- [8] Isakov, S. V., Raman, K. S. , Moessner, R. & Sondhi, S. L. Magnetization curve of spin ice in a [111] magnetic field. *Phys. Rev. B* **70**, 104418 (2004)
- [9] Aoki, H. , Sakakibara, T., Matsuhira K. & Hiroi, Z. Magnetocaloric Effect Study on the Pyrochlore Spin Ice Compound  $\text{Dy}_2\text{Ti}_2\text{O}_7$  in a [111] Magnetic Field. *J. Phys. Soc. Japan* **73**, 2851 (2004).
- [10] Bonner, J. C. & Fisher, M. E. Entropy of an antiferromagnet in a magnetic field. *Proc. Phys. Soc.* **80**, 508 (1962).
- [11] den Hertog, B. C. & Gingras, M. J. P. Dipolar Interactions and Origin of Spin Ice in Ising Pyrochlore Magnets. *Phys. Rev. Lett.* **84**, 3430 (2000).

- [12] Melko, R. G. & Gingras, M. J. P. Monte Carlo studies of the dipolar spin ice model. *J. Phys. Condens. Matter*, **16** R1277-R1319 (2004).
- [13] Isakov, S. V., Gregor, K., Moessner, R. & Sondhi, S. L. Dipolar Spin Correlations in Classical Pyrochlore Magnets. *Phys. Rev. Lett.* **93**, 167204 (2004).
- [14] Isakov, S. V. , Moessner, R. & Sondhi, S. L. Why Spin Ice Obeys the Ice Rules. *Phys. Rev. Lett.* **95**, 217201 (2005).
- [15] Anderson, P. W., Ordering and Antiferromagnetism in Ferrites. *Phys. Rev.* **102**, 1008 (1956)
- [16] Henley, C. L. Power-law spin correlations in pyrochlore antiferromagnets. *Phys. Rev. B* **71**, 014424 (2005).
- [17] Youngblood, R. W. & Axe, J. D. Polarization fluctuations in ferroelectric models *Phys. Rev. B* **23**, 232 (1981).
- [18] Skalyo J, Frazer B. C. & Shirane, G. , Ferroelectric mode motion in  $\text{KD}_2\text{PO}_4$  *Phys. Rev. B* **1**, 278 (1970).
- [19] Harris M. J., Zinkin, M. P., Tun, Z., Wanklyn, B. M. & Swainson, I. P. Magnetic Structure of the Spin-Liquid state in a Frustrated Pyrochlore. *Phys. Rev. Lett.* **73** 189 (1994).
- [20] Ballou, R., Lelièvre-Berna, E. & Fåk, B. Spin Fluctuations in  $(\text{Y}_{0.97}\text{Sc}_{0.03})\text{Mn}_2$ : A Geometrically Frustrated, Nearly Antiferromagnetic, Itinerant Electron System. *Phys. Rev. Lett.* **76**, 2125 (1996).
- [21] Bramwell, S. T. *et al.* Spin correlations in  $\text{Ho}_2\text{Ti}_2\text{O}_7$ : A Dipolar Spin Ice. *Phys. Rev. Lett.*, **87**, 047205 (2001).
- [22] Fennell, T., *et al* Neutron Scattering investigation of the spin ice state in  $\text{Dy}_2\text{Ti}_2\text{O}_7$ . *Phys. Rev. B* **70**, 134408 (2004).
- [23] Moessner, R. & Sondhi, S. L., Theory of the [111] magnetization plateau in spin ice. *Phys. Rev. B* **68**, 064411 (2003).
- [24] Kasteleyn, P. W. Dimer Statistics and Phase Transitions. *J. Math. Phys.* **4**, 287 (1963).

- [25] Petrenko, O. A., Lees, M. R. & Balakrishnan, G. Magnetization process in the spin-ice compound  $\text{Ho}_2\text{Ti}_2\text{O}_7$ . *Phys. Rev. B* **68**, 012406 (2003).
- [26] Tabata, Y. *et al.* Kagome ice state in the dipolar spin ice  $\text{Dy}_2\text{Ti}_2\text{O}_7$ . arXiv:cond-mat/060708 (2006)
- [27] Fennell, T. *et al.* Neutron scattering studies of the spin ices  $\text{Ho}_2\text{Ti}_2\text{O}_7$  and  $\text{DyTi}$  in applied magnetic field. *Phys. Rev. B* **72**, 224411 (2005).
- [28] Mirebeau, I. *et al.* Ordered spin ice state and magnetic fluctuations in  $\text{Tb}_2\text{Sn}_2\text{O}_7$ . *Phys. Rev. Lett.* **94**, 246402 (2005).
- [29] Gardner, J. S. *et al.* Cooperative paramagnetism in the geometrically frustrated antiferromagnet  $\text{Tb}_2\text{Ti}_2\text{O}_7$ . *Phys. Rev. Lett.* **82**, 1012 (1999).
- [30] Lee, S.-H. *et al.* Emergent excitations in a geometrically frustrated antiferromagnet. *Nature* **418**, 856 (2002).
- [31] Lau, G. C., *et al* Zero-point entropy in stuffed spin-ice. *Nature Physics* **2**, 249 (2006).
- [32] Taguchi, Y., Oohara, Y., Yoshizawa, H., Nagaosa, N. & Tokura Y. Spin Chirality, Berry Phase and Anomalous Hall Effect in a frustrated ferromagnet. *Science* **291**, 2573 (2001).
- [33] R. F. Wang *et al* Artificial ‘spin ice’ in a geometrically frustrated lattice of nanoscale ferromagnetic islands. *Nature* **439**, 303 (2006).
- [34] Castro Neto, A. H., Pujol, P. & Fradkin, E. Ice: a strongly correlated proton system. *Phys. Rev. B* **74**, 024302 (2006).
- [35] Limelette, P. *et al.* Universality and Critical Behaviour at the Mott Transition. *Science* **302**, 89 (2003).
- [36] Kutnjak, Z., Petzelt, J. & Blinc, R., The giant electromechanical response in ferroelectric relaxors as a critical phenomenon. *Nature* **441**, 956 (2006).
- [37] Isakov, S. V., Wessel, S., Melko, R. G., Sengupta, K. & Kim, Y. B. Valence Bond Solids and Their Quantum Melting in Hard Core Bosons on the Kagome Lattice. cond-mat/0602430 (2006).

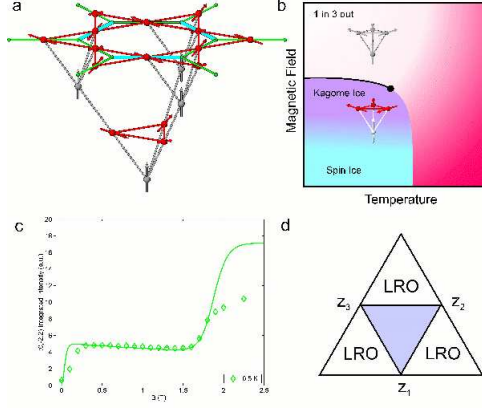


Figure 1: Spin ice and kagome ice. With the trigonal axis ( $[111]$ ) vertical, the pyrochlore lattice can be viewed as stacked kagome planes, separated by interstitial spins forming a triangular lattice (a). In zero field all tetrahedra have a sixfold degenerate groundstate with two spins pointing in and two pointing out (i.e. ice rules), in moderate field this degeneracy is reduced by the pinning of one spin leaving a modified ice rule operating on the three spins in the kagome plane (a and b, lower tetrahedron), in high fields this ice rule is broken and a fully ordered structure with one spin pointing in and three spins pointing out (b, upper tetrahedron) is formed. The transition from kagome ice to long range order shows a liquid-gas critical point in  $\text{Dy}_2\text{Ti}_2\text{O}_7$  [5] and in  $\text{Ho}_2\text{Ti}_2\text{O}_7$  a critical point of unknown type (see main text and Fig. 5). The three phases are distinguished in the magnetic Bragg scattering (c) which shows two plateaux, the first for kagome ice and the second for the fully ordered state. The line is a calculation of the intensity by enumeration of states on a single tetrahedron with field close to  $[111]$ , as described in the text. The tilted field is responsible for the downward trending intensity with field within the kagome ice plateau. Lack of agreement at high fields is attributed to severe extinction at this very intense magnetic Bragg peak. The kagome ice phase can be mapped to the dimer model on a hexagonal lattice by colouring links of the hexagonal lattice located on sites of the kagome lattice with field-opposing spins (a, hexagonal dual lattice in green, dimers in cyan) [23]. The dimer model has a triangular phase diagram with respect to statistical weights of different dimer orientations, the central region corresponds to kagome ice and the lines correspond to Kasteleyn transitions to long range ordered states (LRO) which occur when one dimer orientation outweighs the other two (d).

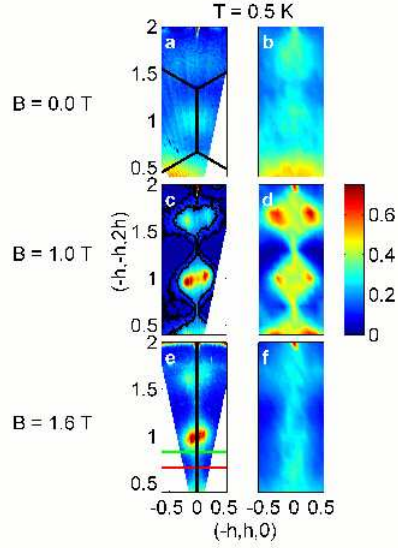


Figure 2: Measured and simulated diffuse scattering in  $\text{Ho}_2\text{Ti}_2\text{O}_7$ . In zero field the experimental diffuse scattering (**a**, 0.0 T, 0.5 K) is only approximately matched by the nearest neighbour spin ice model (**b**), it is anticipated that a dipolar spin ice simulation would be a significant improvement [11,21,26]. In the kagome ice phase (**c**, 1.0 T, 0.5 K) very clear pinch points are observed at  $(\frac{2}{3}, \frac{2}{3}, \frac{4}{3})$  and  $(\frac{4}{3}, \frac{4}{3}, \frac{8}{3})$ . Remarkably the agreement with the nearest neighbour model (**d**) is much improved. The splitting of the central peak is less than that predicted by the simulation and this is ascribed to the tilt. At the termination of the plateau the scattering is localized in a single sharp feature at  $(\bar{1}, \bar{1}, 2)$  (**e**, 1.6 T, 0.5 K) which has the features of an unusual critical point. This behaviour is not captured by the nearest neighbour model (**d**).

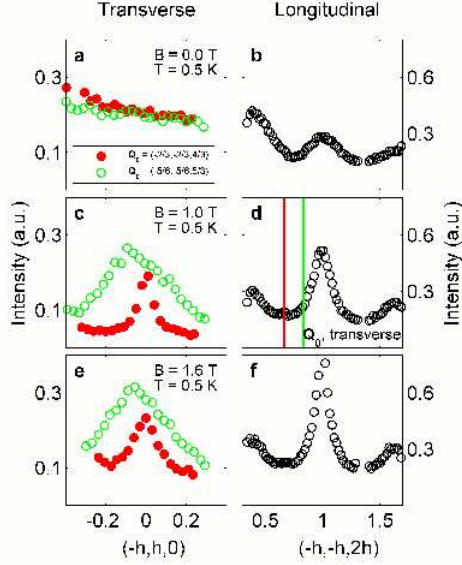


Figure 3: Pinch point scattering. Cuts through the pinch point (the cut positions are illustrated in matching colours in Fig. 2e, all errorbars are smaller than the symbol size) position in zero field (**a,b**) show spin ice scattering and no sharp feature in the transverse cuts parallel to  $(\bar{h}, h, 0)$  (**a**). In 1 T the sharp pinch point has been formed (**c,d**) and also exists in 1.6 T (**e,f**). The pinch point can be seen as the sharp feature in the cut at  $(\bar{h}, h, \frac{4}{3})$ , comparatively broadened at  $(\bar{h}, h, \frac{9}{6})$  and diffuse in the cut along  $(\bar{h}, \bar{h}, 2h)$  where the pinch point position is  $(\frac{2}{3}, \frac{2}{3}, \frac{4}{3})$ . In the longitudinal cuts (**b,d,f**) we also see the developing critical scattering at  $(\bar{1}, \bar{1}, 2)$ .

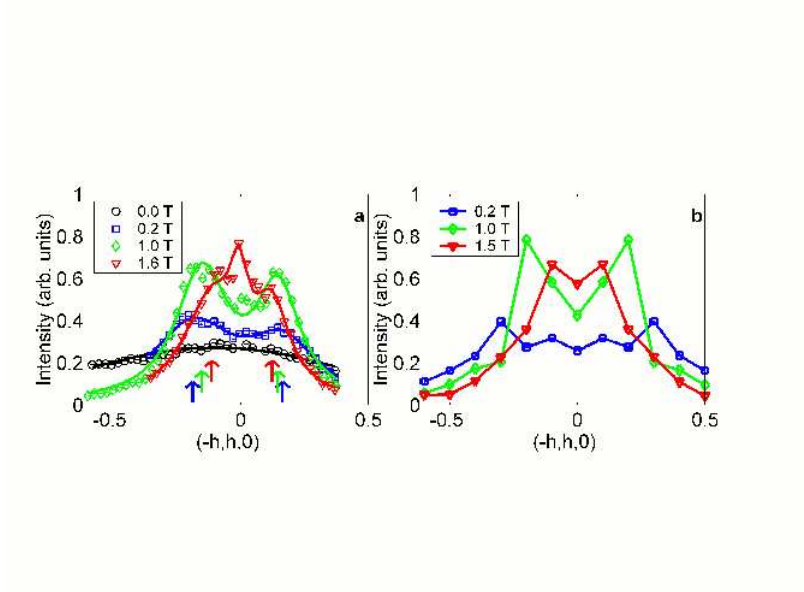


Figure 4: Kasteleyn physics. Cuts through the main scattering feature at  $(\bar{1}, \bar{1}, 2)$  as a function of field show that the broad feature of zero field is replaced by two peaks which drift together as the field is raised across the kagome ice plateau. The experimental data show this process, with the apparent superimposition of the sharp critical like scattering at 1.6 T (**a**), whereas Monte Carlo simulations of the same field scan with a small tilt, show only the drifting peaks as the critical scattering is not reproduced by the nearest neighbour model (**b**). The fitted peak positions in the experimental data are marked below by the arrows.



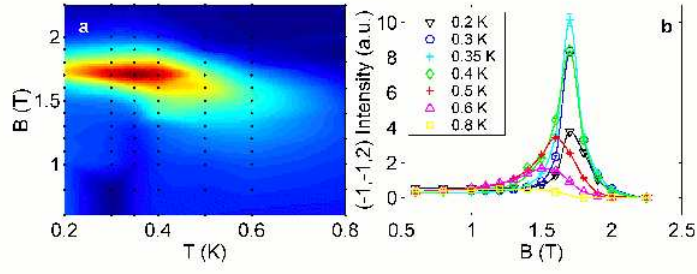


Figure 5: Critical point at plateau termination. The intensity of the critical scattering at  $\bar{1}, \bar{1}, 2$  is strongly dependent on temperature, having a strong maximum at  $T = 0.35$  K and  $B = 1.7$  T, giving the appearance of a critical point. We show the phase boundary in **a** (note the intensity scale is logarithmic) and the detailed behaviour of the intensity in **b**. It is notable that below  $T_c$  the intensity is field independent in the plateau until close to  $B_c$  whereas above  $T_c$  the intensity increases throughout the plateau toward its maximum at  $B_c$ .